Pol. J. Environ. Stud. Vol. 32, No. 2 (2023), 1927-1940
DOI: *10.15244/pjoes/157220* ONLINE PUBLICATION DATE: 2023-02-13

Original Research

Sensitivity Analysis of the Physical Hydrological Model CASC2D-SED in Arid Area

Chuancai Zhang[1]*, Yanyan Ma[2], Chuanwei Zhang[3], Huaipeng Liu[1]

[1]College of Land and Tourism, Luoyang Normal University, Luoyang, Henan 471000, China
[2]The Faculty of Business and Accountancy, Lincoln University College, Petaling Jaya, Selangor Darul Ehsan, 47301, Malaysia
[3]College of Mechanical and Electrical Engineering, Qingdao University, Qingdao, 266071, China

Received: 13 September 2022
Accepted: 6 December 2022

Abstract

Sensitivity analysis of model parameters and inputs is an important research method to improve model accuracy and calibration efficiency. The purpose of this paper is to explore the sensitivity of model parameters and model inputs in arid areas, and then to study the linear or nonlinear relationship of model sensitivity taking Erjiama small watershed in Jungar banner, Ordos, Inner Mongolia, China as the research object. Based on the calibration of CASC2D-SED model, four model parameters, including hydraulic conductivity, Manning coefficient, Suction head and vegetation interception, and one model input-river network were perturbed at a variation rate of 25%. The hydrological process is simulated by using the combination of 20 model parameters and model inputs after perturbation, and then the sensitivity analysis of model parameters and inputs is studied. The results show that: 1) The sensitivity of Manning coefficient to peak discharge and peak arrival time is non-linear, while the sensitivity of hydraulic conductivity, Suction head and vegetation interception to peak discharge, peak arrival time, simulated total discharge and infiltration amount is linear; 2) With the increase of hydraulic conductivity, Suction head and vegetation interception, the peak discharge and simulated total discharge decrease gradually, while the peak arrival time and infiltration amount increase gradually; 3) With the increase of Manning coefficient, the simulated total flow decreases gradually, while the infiltration rate increases gradually; 4) With the increase of the number of tributaries, the peak discharge, the simulated total discharge and the total amount of infiltration gradually decrease, while the flood peak arrival time presents a U-shaped change; 5) With the increase of Manning coefficient, hydraulic conductivity, Interception and Suction head, the simulated sediment flow decreases. Manning coefficient is more sensitive to the simulated amount of clay than the other three model parameters. Sensitivity analysis of parameters and inputs of CASC2D-SED model plays a guiding role in model

*e-mail: zccai1205@163.com

calibration and accurate modeling. This method can be applied to the calibration, structural uncertainty and model application of hydrological models, and has a wide range of application.

Keywords: hydrological process modeling, sensitivity analysis, perturbation method, model input

Introduction

Hydrological modeling is an important tool for water resources management. Hydrological models simulate and predict watershed behavior through model parameters and model inputs. Although the parameters of the physical hydrological model have clear physical meanings and can usually be obtained from actual measurements, the spatial heterogeneity of the surface environment and the simplification of the hydrological processes by the model make the calibration of the parameters of the model inevitable. In order to calibrate the hydrological model more accurately and make the model more accurate, it is necessary to study the sensitivity of hydrological model. Over the years, a great deal of research has been done on the sensitivity of hydrological model parameters at various levels. Sensitivity research of hydrological models involves the application and improvement of sensitivity methods, sensitivity analysis of hydrological models at different scales, sensitivity analysis of different hydrological models, sensitivity analysis of hydrological models under different environments, and the influence of sensitivity of hydrological models on the uncertainty of model structure.

Hou, T tested three sensitivity analysis methods, namely, local sensitivity analysis method SENAN, regional sensitivity analysis method and SOBOL method. Studies show that the selection of analysis method has a certain influence on the sensitivity of Noah's LSM parameters [1]. Song and X. reviewed sensitivity analysis methods [2]. Wang X., on the other hand, studied the sensitivity of distributed hydrological model based on the variational method [3]. Considering that there are more uncertainties in climate models and downscaling processes, the complexity of hydrological modeling system is increased. To address these challenges and improve the performance of hydrological models under climate change conditions, five new methods to support hydrological models are proposed [4]. Global sensitivity analysis method was developed for SWAP-EPIC based on LH-OAT. A modified-MGA based module was developed for global inverse parameter estimation [5]. Stahn, P. evaluated the agricultural hydrological exchange model for simulating soil water balance of different monocropping and mixed crops on the basis of hydrological and phenological observations by using SOBOL global sensitivity method and multi-objective algorithm combination [6]. Singh, V. adopted the parameterization-based sensitivity analysis method to identify the parameters that had the greatest influence on model calibration [7] .

A distributed hydrological model developed for a single mountainous terrain. Morris Screening Method (OAT) and Error Evaluation Calibration Method were combined for Parameter Sensitivity Analysis (PSA) [8]. In the same year, Sheng, S. used the Xin 'anjiang River model to simulate the runoff at different time and space scales in western Jiangxi, Fujian Province, and studied and compared the sensitivity and changes in the basin by using Monte Carlo and SOBOL sensitivity analysis methods respectively [9]. Firstly, qualitative SA method and Morris method were adopted to screen sensitive parameters, and dimensionality reduction of model parameters was carried out. The sensitivity of sensitive parameters was quantitatively quantified using SOBOL method [10]. Liu Haifan improved the hierarchical sensitivity analysis method by defining a new set of sensitivity indicators for the subdivision parameters. A new classification method and Latin hypercube sampling method are proposed to estimate these new sensitivity indicators [11] .

In addition, sensitivity analysis studies of some hydrological models were also carried out according to the characteristics of different study areas [12-14]. According to different hydrological models' needs for parameters and their different physical meanings, it is necessary to analyze the parameter sensitivity of different hydrological models. For example, a parameter sensitivity analysis is performed on these models: MTWRF mode l [15], SWAT [16], MESH model [17], Eurosem model [18], LSM model [19], SLUPR model [20]. Some research achievements have also been made in the parameter sensitivity analysis of hydrological models under different climate conditions [21]. It is of reference significance to analyze the parameter sensitivity of hydrological model under different climate conditions. Some progress has also been made in the study of sensitivity of hydrological models for different study areas [22-26]. In addition, some scholars have studied the sensitivity of hydrological models from different perspectives [27-31].

In conclusion, the parameter sensitivity analysis of hydrological models has achieved good results; however, there are still a lot of problems worth studying. The sensitivity of physical hydrological models in arid areas has not been studied deeply in the existing literature. In this study, the parameter sensitivity and model input sensitivity of physical hydrological model CASC2D-SED in the hydrological simulation of desert areas in North China were analyzed. Sensitivity analysis is used to improve the accuracy of hydrological model parameters and determine appropriate model inputs, so as to provide theoretical support for improving the accuracy and efficiency of hydrological simulation

and prediction. Aiming at the characteristics of river network dynamic change in the simulation of physical hydrological process in arid area, the breakthrough of this paper is to explore the sensitivity of river network to the model in the arid area.

Materials and Methods

Study Site and Numerical Model

Study Site

Erjiama small watershed (Fig. 1) is located in Shage Du Town, Jungar Banner, Inner Mongolia Autonomous Region, China. It is a first-class tributary of Huangfuchuan watershed, with a total area of 50.3 km^2. Its geographical coordinates are 110°47‘35.7“E and 39°41’54.9”N. The elevation is between 1113-1267 m, and the relative elevation difference is 154 m. The basin strata are mainly composed of Mesozoic Triassic, Jurassic and Cretaceous sandstone, conglomerate and mudstone interbedded (commonly known as arsenic sandstone). There are three types: one is brown-red silty sandstone; the second is grayish white sandstone; The third is pink-white sandstone.

Erjiama small watershed is a typical gravel hilly gully region. The slope of the ground is 5~25 degrees, and the maximum slope of the gully slope is 45 degrees. The shape of the channel is “U” shape, and the upper reaches of the furrow are “V” shape. The terrain is broken, the gullies are wide and widely developed, and the average gully density is 2.2 km/km^2. The surface soil is mainly loess and millet calcium soil with uneven thickness. Due to human activities and overgrazing, the surface vegetation has been seriously damaged. The average annual temperature in this basin is 60~90 mm, and the average annual precipitation is 375~453.5 mm.

The main crops of the basin are corn, beans, millet, yam and so on. The cultivated land area is 386.7 hm^2, accounting for 7.69% of the total area, including 107.6 hm^2 of terraces and terraces. Forestland covers an area of 1991 hm^2, accounting for 39.58% of the total area. In the river basin, the artificial shrubs of caragana korshinskii and sea-buckthorn are mainly found on the top of the ridge and mole and on the banks of the gully slope, and the arbor forests are distributed in small patches along each branch of the gully and along both sides of the Rongwu Expressway. The forbidden area is 301.6 hm^2, accounting for 6.0% of the total land area. The area of wasteland and hard-to use land in the small watershed is 2350.7 hm^2, accounting for 46.73% of the total land area, which is distributed on exposed arsenic sandstone gully slope and steep gully slope in the small watershed. Most of them are wasteland after the implementation of ecological restoration projects in recent years. The artificial grassland is scattered on the gentle slope and the converted slope in the middle and lower reaches.

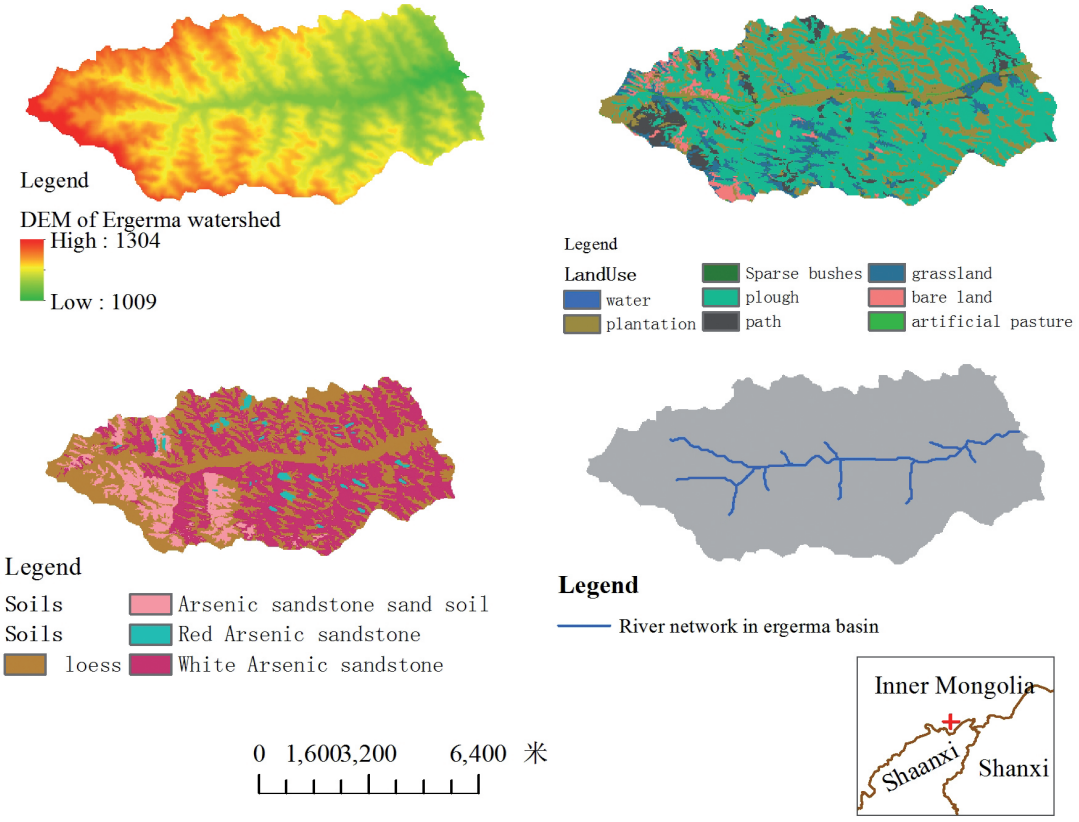

Fig. 1. Model input data for Ergerma watershed.

Numerical Model

The mathematical model adopted in this study is CASC2D-SED model, and the hydrological process simulated by CASC2D-SED model includes hydrological process and sediment process. Hydrological processes include rainfall process, vegetation closure process, soil infiltration process, slope runoff process, channel runoff process, base flow and surface water storage process. The sediment process includes slope erosion process, slope sediment migration process, slope sediment deposition process, channel sediment deposition process and channel sediment migration process. The CASC2D-SED model uses the approximation of Green and Ampt equations to describe the infiltration process. In particular, this relationship is used as a component to generate overland flow in the model infiltration simulation scheme to determine soil infiltration depth and infiltration rate. Ignoring the surface water level, the basic equation of Green-Ampt relationship is as follows:

$$f = Ks\left(1 + \frac{H_f M_d}{F}\right) \tag{1}$$

Where, f is infiltration rate, Ks is saturated hydraulic conductivity, H_f is the capillary Suction head at the wetting peak, M_d is the soil water shortage, $M_d = (q_e\text{-}q_i)$, q_e is the effective porosity, $q_e = j\text{-}q_r$, J is the total soil porosity, q_r is residual saturation, q_i is the initial soil moisture content, F is the total infiltration depth.

Continuity equation and momentum equation of Saint Venant equation are used as governing equations of overland flow simulation. Using these equations, the CASC2D-SED model uses finite difference and diffused waves to calculate the overland flow. These equations are usually described in the form of partial differential equations. The continuity equation is:

$$\frac{\partial h_0}{\partial t} + \frac{\partial q_x}{\partial x} + \frac{\partial q_y}{\partial y} = e \tag{2}$$

Where, h_o is the depth of surface runoff, q_x and q_y are the single-width flow in the direction of x and y respectively, e is Super permeable rainfall, the two-dimensional diffusion fluctuation equation is:

$$S_{fx} = S_{ox} - \frac{\partial h_0}{\partial x} \tag{3}$$

$$S_{fy} = S_{oy} - \frac{\partial h_0}{\partial y} \tag{4}$$

In the formula, S_{ox} and S_{oy} are respectively slope drops in x and y directions, S_{fx} and S_{fy} are respectively slope bottom friction drops in x and y directions.

The channel runoff process is calculated by one dimensional explicit finite difference method with diffusion wave. The continuity equation is:

$$\frac{\partial A}{\partial t} + \frac{\partial Q}{\partial x} = q_0 \tag{5}$$

Where: A is the sectional area of water flow, Q is river discharge, q_0 is the lateral inflow or outflow. One-dimensional diffusion wave equation:

$$\frac{\partial y}{\partial x} = i_0 - i_f \tag{6}$$

In the formula, i_0 refers to the slope of river bottom, i_f is friction slope, y is the depth of the river bottom.

The model includes surface erosion and sediment transport processes. The soil particles are denuded at the surface and moved down with the current. The supply capacity of erosion material and the migration capacity of river are two opposing factors controlling erosion rate. The typical case is that fine sediment can be carried away in large quantities by the current and therefore has a limited supply capacity. Coarse-grained soil is more difficult to be carried away by water flow, so the coarse-grained soil has a limited movement rate due to the limitation of water migration capacity. The total volume of sheet erosion and rill erosion in bare soil is calculated by the improved Kilinc & Richardson equation. The improved KR (Kilinc & Richardson) equation takes into account soil type, vegetation cover type and K, C and P factors of USLE. For an pixel with a size of dx meters and a time interval of dt seconds, the formula for calculating the erosional matter volume in the pixel is as follows:

$$\forall_{S_{kR}} = 58390 * S_0^{1.664} * q^{2.035} * K * C * P * dx * dt \tag{7}$$

The calculation formula for the volume of suspended matter with particle size i transported by advection is as follows:

$$\forall S_{sus_i} = SusVol_i * \frac{V * dt}{dx} \tag{8}$$

In the formula, V is the river basin, m/s, S_{susi} is the volume of suspended particles with particle size i, cubic meters. The volume of suspended matter with particle size i from the source pixel to the receiving pixel is the maximum of both the volume of advection migration erode and the volume of erode calculated by the KR equation. The calculation equation is as follows:

$$\forall S_{SUS_i} == \begin{cases} MAX\left(SusVol_i * \frac{Vdt}{dx};\ \forall S_{KR} * \frac{SusVol_i}{\sum_{i=1}^{3} SusVol_i}\right), & \forall S_{KR} < \sum_{i=1}^{3} SusVol_i \\ SusVol_i, & otherwise \end{cases} \tag{9}$$

The runoff transport capacity is reduced due to the transport of suspended sediment, and the remaining runoff transport capacity is calculated by the following formula:

$$totXSScap = \mathrm{MAX}\left(0;\ \forall S_{KR} - \sum_{i=1}^{3} S_{sus_i}\right) \quad (10)$$

The remaining runoff transport capacity is used to transport sand bed erosion. The formula for calculating the volume of erosion with particle size I from the source pixel to the receiving pixel is as follows:

$$\forall S_{BM_i} = \begin{cases} totXSScap * \frac{BMVOl_i}{\sum_{i=1}^{n3} BMVOl_i}, & totXSScap < \sum_{i=1}^{3} BMVOl_i \\ \sum_{i=1}^{n3} BMVOl_i\ ,\ otherwise \end{cases} \quad (11)$$

$BMvol_i$ is the volume of sand bed erosion with particle size i in the source pixel, cubic meters. Once both suspended and sand-bed erosions have been migrated, if a certain migration capacity is still retained, this part of the erosional migration force will erode the soil parent material. Soil parent material is eroded in proportion to grain size. The calculation formula of erosion volume is as follows:

$$\forall S_{EROS_i} = \left(totXSScap - \sum_{i=1}^{3} Qs_{BM_i}\right) * P_i \quad (12)$$

In the formula, P_i is the proportion of erosion material in soil parent material.

The model includes channel sediment transport processes. The CASC2D-SED model does not allow river erosion and has certain limitations, but the model allows sediment deposition. Sediment transport capacity of river course is calculated by Engelund and Hansen equations, which are as follows:

$$\forall S_{EH_i} = \frac{Q * Cw_i * dt}{2.65} \quad (13)$$

Where, Q is river runoff, cubic meters/second, Cw_i is the weight concentration of sediment with particle size i. The calculation formula for the volume migration of suspended solids with particle size i by advection in the river channel is as follows:

$$\forall S_{SUS_i} = SusVol_i * \frac{Vdt}{dx} \quad (14)$$

The remaining runoff migration capacity is used to transport sand bed materials, and the calculation formula for the volume of sand bed materials with a particle size of i is as follows:

$$\forall chi = BMVOl_i * \frac{Vdt}{dx} \quad (15)$$

If there is still residual runoff migration capacity, it is no longer used.

The model includes the suspended sediment deposition process. Sediment is allowed to be deposited on both slopes and channels, and it is assumed that particles do not interact with each other and deposit independently. The calculation formula of the deposition ratio Psi with the particle size of sediment i is as follows:

$$P_{si} = \begin{cases} W_i * \frac{dt}{h}, h > W_i dt \\ 1,\ \ h \le W_i dt \end{cases} \quad (16)$$

Where, W_i is the estimated deposition velocity of suspended sediment particles with a median particle size of i, m/s, h is the depth on the pixel, meters.

Data Sources

The data needed in this study include topographic data, land use data, soil characteristics data, rainfall data and runoff monitoring data. Topographic data uses GDEMV2 30M resolution digital elevation data, which comes from China Geospatial Data Cloud. Land use data are derived from remote sensing visual interpretation of remote sensing images of earth maps. Soil characteristic data were obtained from field measurement, field sampling and laboratory analysis. The rainfall data were obtained from the automatic rain gauge of the meteorological station in the study area. Runoff monitoring data were obtained from field manual monitoring in the research area by the Water Conservation Bureau of Junge Banner, Inner Mongolia, China.

Method of Disturbance Analysis of Sensitivity Analysis

The sensitivity disturbance analysis of CASC2D-SED of physical hydrological model firstly requires the acquisition and processing of the data in the study area, and then the model calibration. Thirdly, the model data is disturbed according to 25% and the disturbed data is input into the model. Fourthly, the disturbance analysis is performed on the simulation results, and the fifth, the river network structure data of multiple levels in the study area is dynamically extracted. Multiple levels of river network data were input into the calibrated model to simulate the hydrological process, and the influence of the change of river network structure on the hydrological process was studied. The technical flow chart of this paper is Fig. 2.

Model Calibration of CASC2D-SED

Based on the hydrological process simulation of Erjiama small watershed, soil samples and soil water content were collected, soil particle composition was analyzed, and soil hydraulic conductivity and soil water content data were calculated. On this basis,

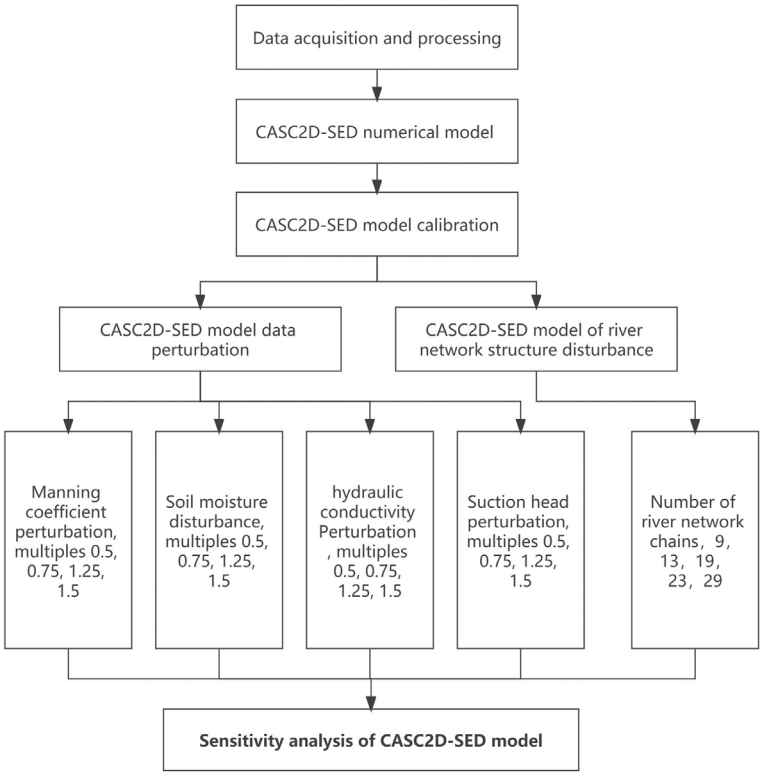

Fig. 2. The technical flow chart of this paper.

CASC2D-SED model was calibrated based on two rainfall events. The model calibration method adopts the trial-and-error method. After more than ten times of trial and error for each parameter, the model parameters of the hydrological process in Erjiama small watershed are determined (Table 1, Table 2). The model parameters are used as the basis points for subsequent parameter perturbation. According to the calibration of a rainfall on June 30, 2014, the actual peak flood flow was 15.748 m^3/s, and the simulated flow of the calibration model was 14.68 m^3/s, with an accuracy of 93.27%.

Disturbance Calculate of Sensitivity Analysis of CASC2D-SED

The parameters of the model calibration in Section 2.2.1 are perturbed. The perturbing method is to perturb at a ratio of 25%. Based on the result of the perturbation, the hydrological process is simulated. The specific perturbation scheme is to perturb only one parameter at a time, and the perturbation of this parameter is 0.5, 0.75, 1.25 and 1.75 times of the original calibration parameter at a ratio of 25%. Therefore, a model parameter needs to be perturbed for four times, and accordingly, four times of hydrological process simulations are needed.

Table 1. Parameters of Land Use Types in CASC2D-SED Model.

Land Use Index	Land Use Type	Manning n [--]	Interception [mm]	CUSLE [--]	PUSLE [--]
1	Grassland	0.013	1.4	0.036	1
2	Artificial pasture	0.013	1.2	0.01	1
3	Sparse bushes	0.015	1.6	0.018	1
4	Bare land	0.011	1.1	0.072	1
5	Plantation	0.02	2.5	0.036	1
6	Path	0.005	0.6	0.018	1
7	Plough	0.016	0.9	0.018	1
8	Water	0.001	0.1	0.01	1

Table 2. Parameters of Soil Types in CASC2D-SED Model.

Soil Type	Soil Index	Hydr. Cond. [cm/h]	Suction head [cm]	Moisture Deficit [cm^3/cm^3]	Sand [%]	Silt [%]	Clay [%]	KUSLE [--]
Loess	1	0.134	35	0.013	0.115	0.645	0.24	0.1
Arsenic sandstone sand	2	0.242	32	0.012	0.145	0.614	0.24	0.1
White Arsenic sandstone	3	0.114	28	0.01	0.165	0.608	0.23	0.1
Red Arsenic sandstone	4	0.114	29	0.01	0.159	0.618	0.22	0.1

Respectively on the manning coefficient, amount of vegetation intercept, hydraulic conductivity, Suction head and soil moisture, we perturbed it four times, separately corresponding hydrological process simulation. A model parameter is perturbed for 4 times, and the 5 parameters are perturbed for 20 times in total. 20 hydrological process simulations are carried out accordingly. The corresponding simulation results of each model after disturbance are shown in Table 3, Table 4, Table 5, Table 6 and Table 7.

In addition to the influence of model parameters on the hydrological process, the model input also has a very important influence on the hydrological process. For small watershed in arid area, river network changes with precipitation process and runoff production process, and the expression of river network is also uncertain, so the expression of river network has a certain influence on the hydrological process. Four levels of river network were extracted according to the runoff accumulation amount of 2000, 2500, 300, and 3500 (Fig. 3). On the basis that the basic parameters of model calibration in Section 2.2.1 remain unchanged, the river network level is changed and the hydrological process is simulated for four times respectively. The simulated hydrological process results are shown in Table 8.

Results and Discussion

Analyst of Sensitivity of Model Parameters

According to the hydrological process simulation results after the disturbance of each model parameter, the change curves of four flood peaks corresponding to the disturbance of Manning coefficient, interception, conductivity, suction head are respectively drawn (Fig. 4). The change curves of arrival time of four flood peaks (Fig. 5). According to Fig. 4, the change curve of the peak discharge corresponding to the disturbance of Manning coefficient shows a nonlinear relationship, while the change curve of the interception hydraulic conductivity and the suction head shows a linear

Table 3. The simulation results corresponding to Manning coefficient perturbation.

Manning system perturbation multiple	Peak discharge (m^3/s)	Peak arrival time (min)	Simulation of runoff quantity (m^3)	The total amount of river closure (m^3/s)	Infiltration amount (m^3)
0.5	20.24	69.53	96921.02	1119271.13	335494.2
0.75	15.94	52.81	92618.15	1119271.13	349196.4
1	14.68	54.5	89180.43	1119271.13	359500.8
1.25	13.68	55.95	86199.35	1119271.13	368016.5
1.5	12.82	57.25	83609.1	1119271.13	375439

Table 4. The simulation results corresponding to Vegetation interception perturbation.

Interceptor perturbation multiple	Peak discharge (m^3/s)	Peak arrival time (min)	Simulation of runoff quantity (m^3)	The total amount of river closure (m^3/s)	Infiltration amount (m^3)
0.5	15.14	54.19	93617.8	1153830.38	363750.5
0.75	14.92	54.33	91403.75	1136345.38	361616.2
1	14.68	54.5	89180.43	1119271.13	359500.8
1.25	14.43	54.71	86932.88	1102122.75	357423.7
1.5	14.16	54.94	84694.67	1083773	355531.4

Table 5. The simulation results corresponding to Vegetation interception perturbation.

Perturbation multiple of hydraulic conductivity	Peak discharge (m^3/s)	Peak arrival time (min)	Simulation of runoff quantity (m^3)	The total amount of river closure (m^3/s)	Infiltration amount (m^3)
0.5	15.87	53.96	103484.88	1119271.13	258908.9
0.75	15.24	54.23	95774.77	1119271.13	313291.4
1	14.68	54.5	89180.43	1119271.13	359500.8
1.25	14.15	54.78	83389.77	1119271.13	400022
1.5	13.65	55	78156.48	1119271.13	435944.5

Table 6. Tthe simulation results corresponding to Suction head perturbation.

Suction head perturbation multiple	Peak discharge (m^3/s)	Peak arrival time (min)	Simulation of runoff quantity (m^3)	The total amount of river closure (m^3/s)	Infiltration amount (m^3)
0.5	15.46	54.1	96523.23	1119271.13	307948.9
0.75	15.04	54.31	92514.66	1119271.13	336003.6
1	14.68	54.5	89180.43	1119271.13	359500.8
1.25	14.36	54.68	86249.84	1119271.13	380011.4
1.5	14.07	54.86	83643.68	1119271.13	398391.7

Table 7. The simulation results corresponding to soil humidity perturbation.

Soil moisture disturbance factor	Peak discharge (m^3/s)	Peak arrival time (min)	Simulation of runoff quantity (m^3)	The total amount of river closure (m^3/s)	Infiltration amount (m^3)
0.5	15.46	54.1	96523.23	1119271.13	307948.9
0.75	15.04	54.31	92514.66	1119271.13	336003.6
1	14.68	54.5	89180.43	1119271.13	359500.8
1.25	14.36	54.68	86249.84	1119271.13	380011.2
1.5	14.07	54.86	83643.68	1119271.13	398391.8

relationship. And their linear rate of change from large to small is the flood peak change curve corresponding to hydraulic conductivity, suction head and interception. That is, the sensitivity of the model parameters to the peak discharge, the sensitivity of the hydraulic conductivity is greater than the sensitivity of suction head, and the sensitivity of suction head is greater than the interception. The sensitivity of Manning coefficient disturbance to peak discharge increases sharply with the decrease of Manning coefficient. When it is greater than the fixed parameter, the sensitivity of the Manning coefficient to the peak flow decreases linearly with the increase of the Manning coefficient, but the speed of its reduction is still greater than that of the other three model parameters. In conclusion, Manning coefficient is the most sensitive model parameter to peak flow. According to Fig. 5, the Manning coefficient presents a V-shaped change with respect to the flood peak arrival time, that is, it decreases first and then increases. When the Manning coefficient is less than the constant value, it shows a sharp decrease trend, while when it is greater than the constant value, it shows a slow increase trend. According to Fig. 5, the influence of Manning coefficient on the flood peak arrival time shows that the flood peak has the fastest arrival time. According to Fig. 5, the influences of hydraulic conductivity interception and Suction head on flood peak reaching time are positively correlated with the increase of multiples. In other words, the peak arrival time increases with the increase of the hydraulic conductivity interception and the suction head. For the increasing rate of the peak arrival time, the influences of the hydraulic conductivity is greater than the interception, and it is greater than the suction head, that is, the sensitivity of the hydraulic conductivity is greater than the interception and it is greater than the suction head.

According to Fig. 6, Manning coefficient suction head interception and hydraulic conductivity are negatively correlated with the simulated flow, that is, with the increase of the four model parameters, the simulated flow decreases gradually. According to

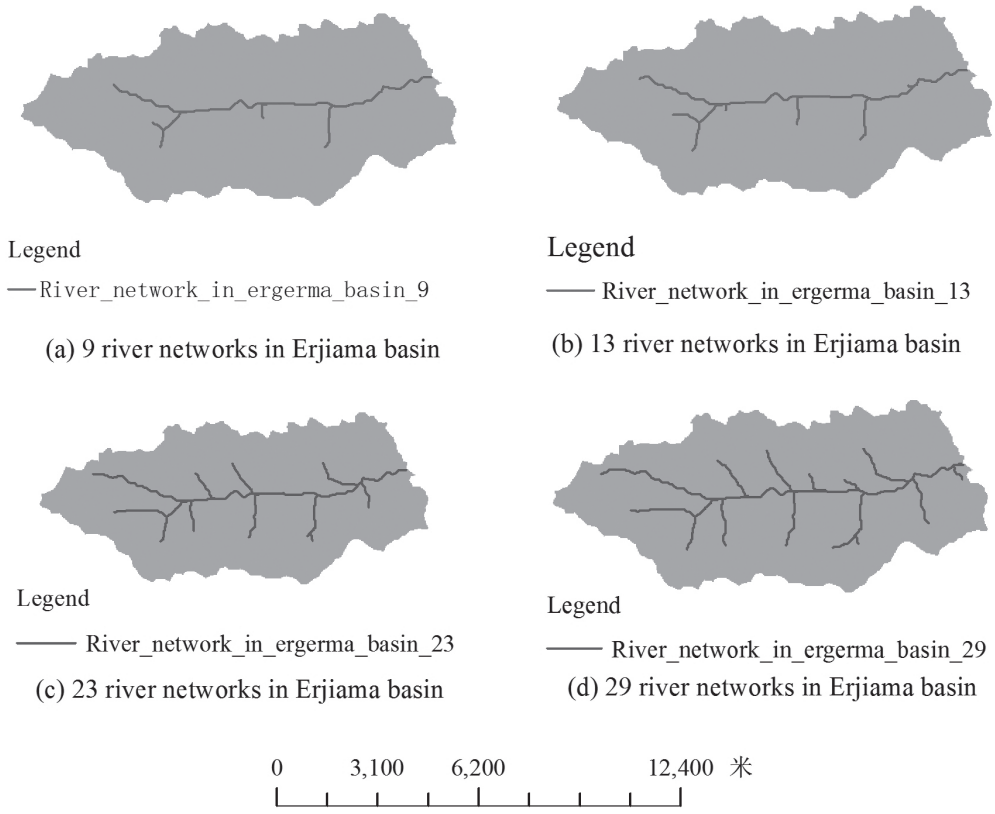

Fig. 3. Model drainage density data for Ergerma watershed.

Table 8. the simulation results corresponding to Drainage density perturbation.

Number of river network chains	Peak discharge (m^3/s)	Peak arrival time (min)	Simulation of runoff quantity (m^3)	The total amount of river closure (m^3/s)	Infiltration amount (m^3)
9	19.9	82.01	138935.84	1119271.13	369730.4
13	14.85	54.64	104450.51	1119271.13	366850.5
19	14.68	54.5	89180.43	1119271.13	359500.8
23	14.68	54.5	89648.41	1119271.13	355213
29	4.3	97.52	33566.2	1119271.13	348338.7

Fig. 6, for the simulated flow, the sensitivity of the Suction head is greater than the hydraulic conductivity is greater than the Manning coefficient and greater than the interception. According to Fig. 7, with the increase of the Manning coefficient of hydraulic conductivity and Suction head, the total amount of infiltration increases, and with the increase of the amount of interception, the total amount of infiltration decreases. Among them, the hydraulic conductivity is the most sensitive to the total amount of infiltration, which is consistent with our cognition. With the increase of hydraulic conductivity, the speed of infiltration accelerates, and the total amount of natural infiltration increases. According to Fig. 7, from the perspective of sensitivity alone, the sensitivity of hydraulic conductivity is greater than that of suction head is greater than that of Manning coefficient, and interception is greater.

According to the simulation results based on four model parameters including Manning coefficient, interception, hydraulic conductivity and pressurized head, which were perturbed up and down for four times at a variation rate of 25%, the variability curves of the simulated fine sand, silt and clay flowing out of the drainage basin with the perturbation of model parameters were drawn (Fig. 8, Fig. 9, Fig. 10, and Fig. 11). According to Figure 8, the simulated sediment flow corresponding to the disturbance of Manning coefficient showed a downward trend, and the simulated clay and total sediment amount decreased rapidly with the increase of Manning coefficient, forming a concave curve. However, with the increase of Manning coefficient, the simulated fine sand quantity does not

decrease quickly, while the simulated fine sand quantity decreases linearly with the increase of Manning coefficient. According to Fig. 9, the simulated fine sand amount, silt amount and clay amount decrease linearly with the increase of the interception parameter, in which the simulated fine sand amount is very small and far lower than the simulated silt brightness and clay

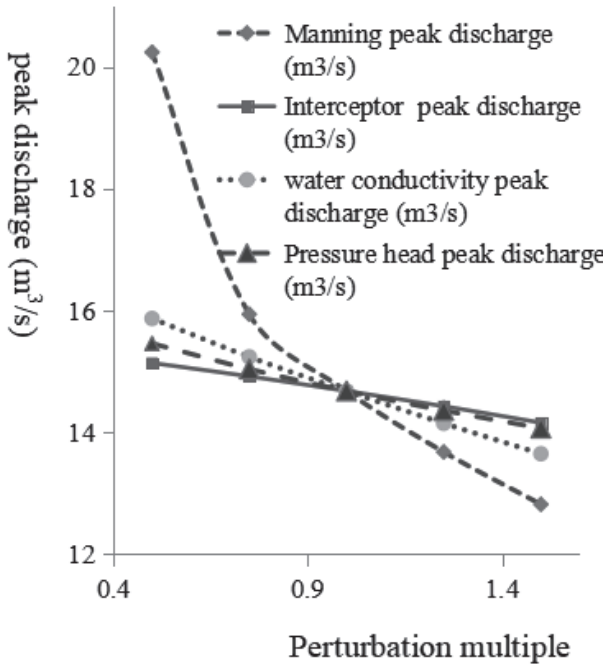

Fig. 4. Influence of Manning coefficient, interception, hydraulic conductivity and Suction head disturbance on peak discharge.

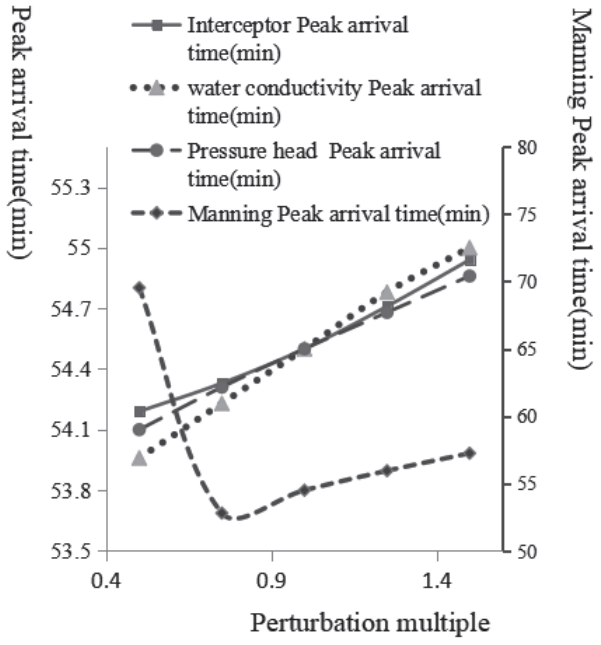

Fig. 5. Influence of Manning coefficient, interception, hydraulic conductivity and Suction head disturbance on peak arrival time.

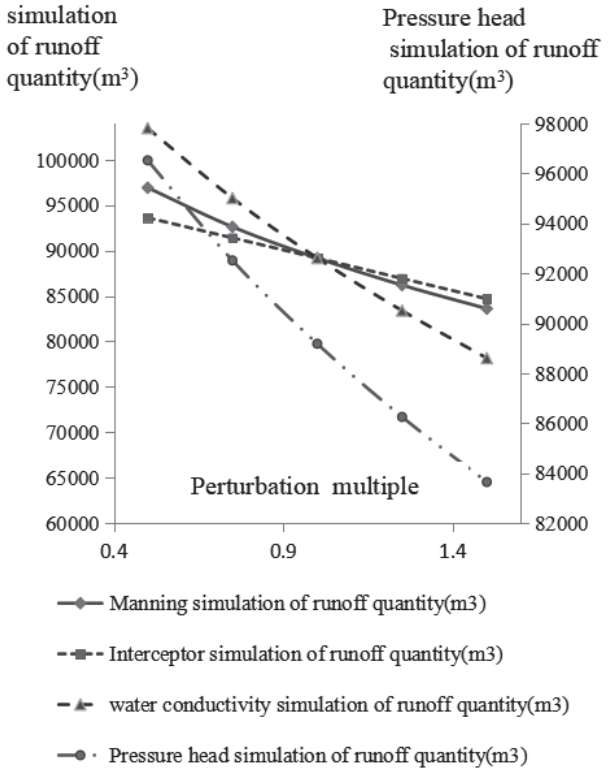

Fig. 6. Influence of Manning coefficient, interception, hydraulic conductivity and Pressure head simulation of runoff quantity.

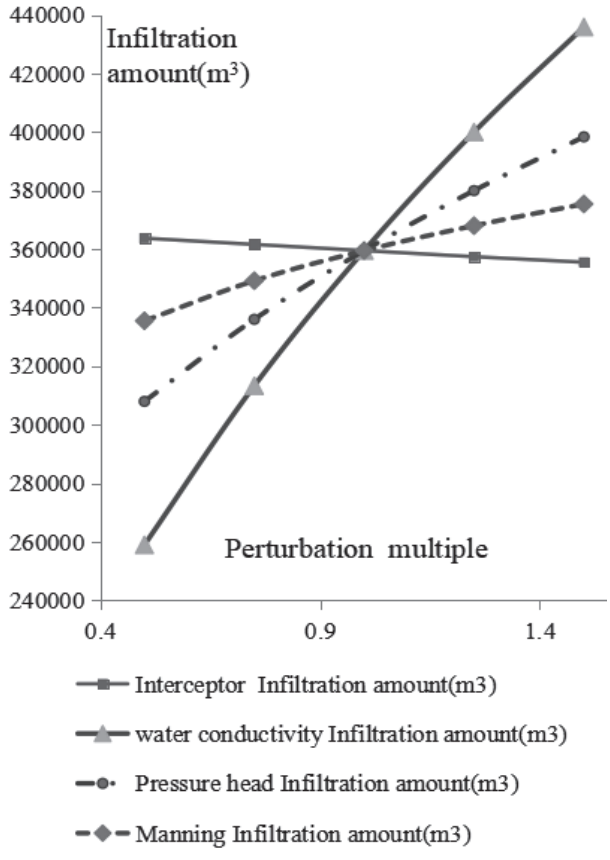

Fig. 7. Influence of Manning coefficient, interception, hydraulic conductivity and Suction head disturbance on infiltration.

amount. According to Fig. 10, the simulated amount of fine sand is small, but decreases rapidly with the increase of hydraulic conductivity, while the simulated amount of silt is lower than that of clay and the change rate is small. According to Fig. 11, the simulated fine sand amount is very small, but it changes rapidly and decreases rapidly with the increase of Suction head. According to Figs 8, 8, 9 and 10, compared with Manning coefficient and interception, hydraulic conductivity and Suction head are more sensitive to the simulated fine sand amount. Compared with interception and Suction head, Manning coefficient and hydraulic conductivity are more sensitive to the simulated clay amount.

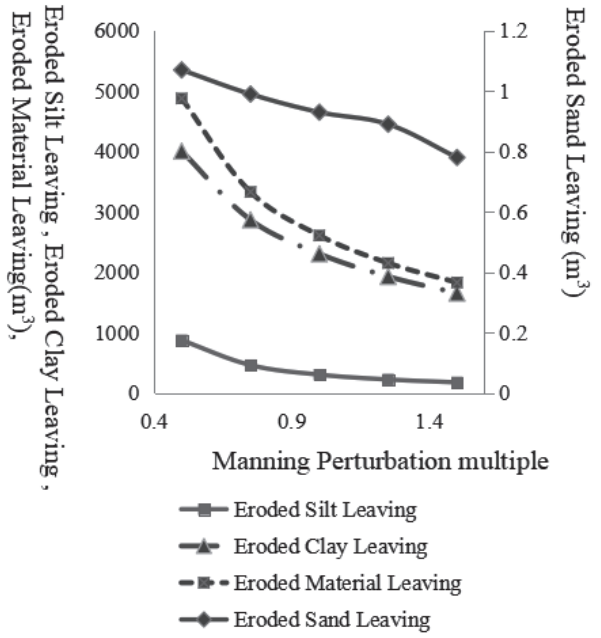

Fig. 8 Influence of manning perturbations on Eroded Silt Leaving Watershed.

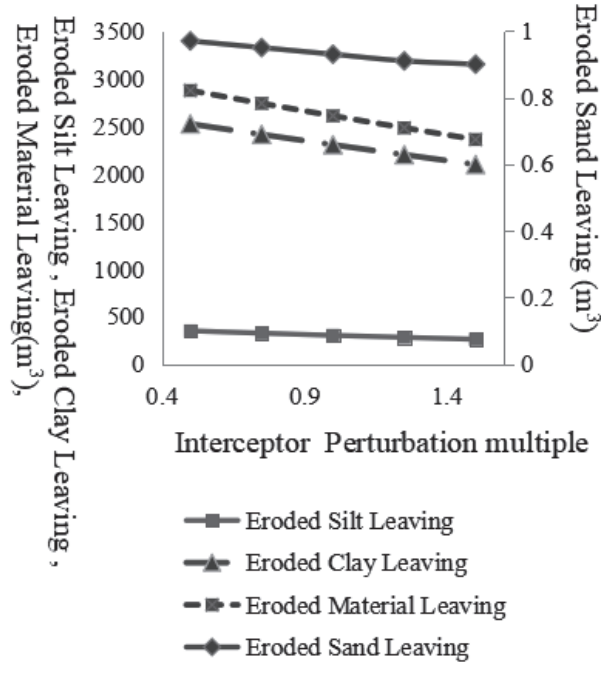

Fig. 9. Influence of interceptor perturbations on Eroded Silt Leaving Watershed.

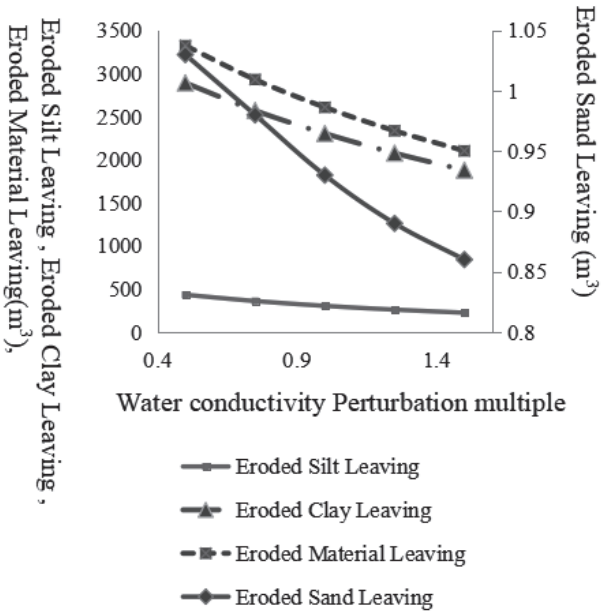

Fig. 10. Influence of hydraulic conductivity perturbations on Eroded Silt Leaving Watershed.

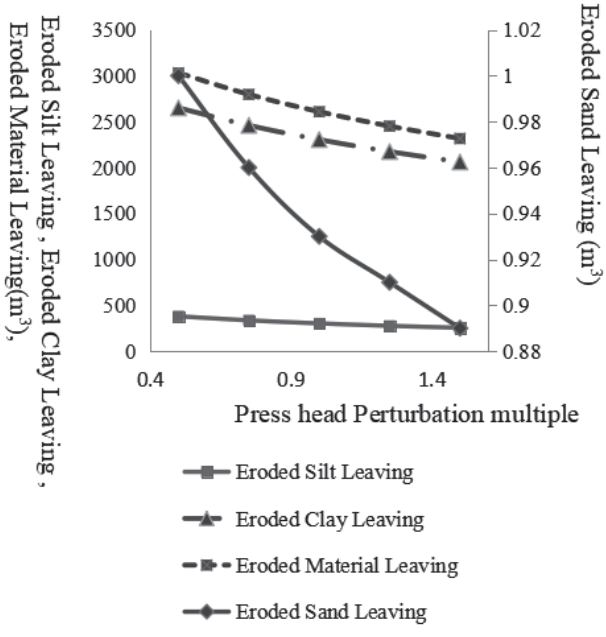

Fig. 11. Influence of suction head perturbations on Eroded Silt Leaving Watershed.

Analyst of Sensitivity of Model Inputs

For arid areas, river network is generated dynamically during rainfall, and as a model input, river network has a certain influence on the simulation results. The data of the river network containing 9, 13, 19, 23 and 29 tributaries in the study area were extracted and put into the model for calculation respectively to draw the change curve between the number of tributaries in the river network and the hydrological simulation results (Fig. 12). According to Fig. 12, the simulated total flood peak discharge and total infiltration decrease with the increase of the number of tributaries in the river network, but the flood peak arrival time presents a U-shaped change with the increase of the number of tributaries in the river network. According to Figure 8, when there are 13, 19 and 23 tributaries in the river network, the flood peak arrival time is relatively stable. However, when there are 9 tributaries in the river network and 29 tributaries in the river network, the flood peak arrival time is relatively late.

According to the number of tributaries of the extracted river, the hydrological process was simulated for five times and the sensitivity curve of the simulated sediment amount to the number of tributaries of the river was drawn (Fig. 13). According to Fig. 12, the simulated fine sand amount is small and decreases with the increase of river tributaries, and the change curve is concave. The simulated fine sand amount is relatively stable when the river tributaries are around 19 and 23. According to Fig. 12, the simulated clay amount is much higher than the simulated silt amount and fine sand amount, and decreases rapidly with the increase of the tributaries of the river. When the number of tributaries is greater than or equal to 23, the simulated clay amount decreases slightly. According to Fig. 12, the simulated silt amount decreases with the increase of river tributaries, but the decreasing rate is significantly less than that of clay amount with the increase of river tributaries.

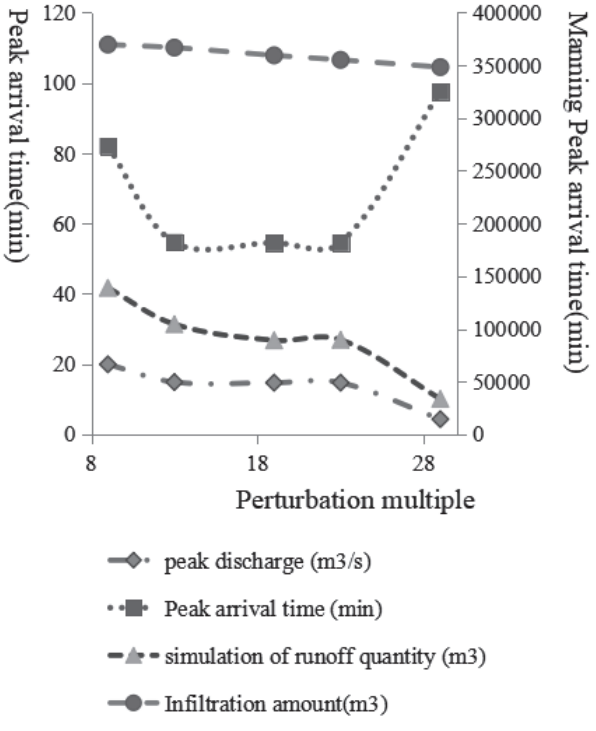

Fig. 12. Influence of drainage density on peak discharge, peak arrival time, simulation of runoff quantity and infiltration.

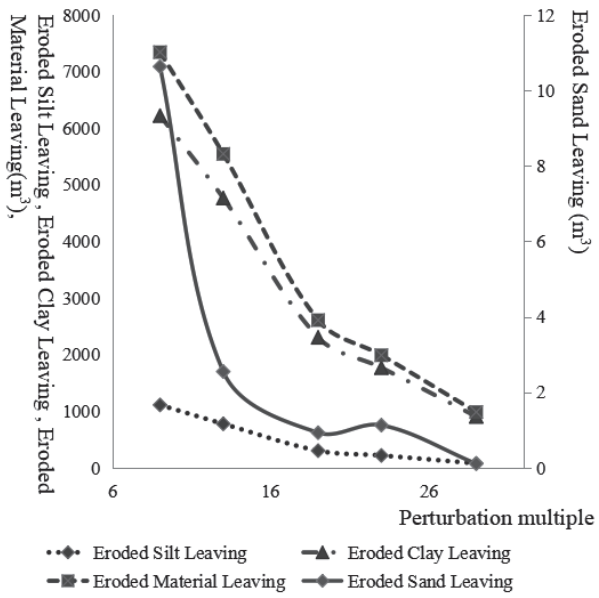

Fig. 13. Influence of drainage density on Eroded Silt Leaving Watershed.

Discussion

According to Fig. 4, Fig. 5, Fig. 6, Fig. 7 and Fig. 8, we obtained the sensitivity curve of model parameters, which has important reference value for model calibration and can improve the efficiency of model calibration. However, each model parameter has certain physical significance, that is, it can be obtained through actual measurement. The measured values of a model's parameters in different locations have certain differences, which is also the reason for the need for model calibration. The model does not adopt real distributed data, but generalizes it. It should not seriously exceed the measured value range. The effect of Manning coefficient on peak discharge and peak arrival time is nonlinear, so the calibration of Manning coefficient is the most difficult.

Conclusions

The CASC2D-SED model parameters were calibrated according to the two rainfall events on June 30 and August 22, 2014, and then on the basis of the calibrated parameters, the Manning coefficient,

hydraulic conductivity, Suction head and interception were disturbed at the rate of 25% variation, as well as the river network was disturbed. Based on the model parameter perturbation and the river network perturbation, the hydrological process was simulated, and then the sensitivity of the model parameters and the model input-river network was analyzed. Sensitivity analysis showed that: 1) The sensitivity curve of Manning coefficient to peak discharge and peak arrival time shows a nonlinear relationship and changes sharply in the range below the fixed value. The sensitivity of Manning coefficient to flood peak flow changes sharply and to flood peak arrival time changes slowly when the rate is higher than the fixed value. Therefore, it is difficult to determine the Manning coefficient of flood peak discharge and flood peak arrival time. 2) There is a linear relationship between the sensitivity of hydraulic conductivity rate, Suction head and interception to the total amount of seepage under simulated flow at the time of flood peak arrival, which is easy to be calibrated. 3) The peak flow rate and simulated total flow rate decrease with the increase of Manning coefficient hydraulic conductivity interception and Suction head. 4) The peak arrival time and total infiltration amount increase with the increase of hydraulic conductivity, interception and Suction head. 5) The peak discharge, the simulated total discharge and the total infiltration decrease with the increase of the number of tributaries in the river network, and the flood peak arrival time presents a U-shaped change with the increase of the number of tributaries in the river network. 6) With the increase of Manning coefficient, hydraulic conductivity, Interception and Suction head, the simulated sediment flow decreases. Manning coefficient is more sensitive to the simulated amount of clay than the other three model parameters. The sensitivity analysis of model parameters and model input-river network to hydrological process simulation can be used as a guide for model parameter calibration and accurate watershed modeling.

Acknowledgments

The present work is funded by National Science-technology Support Plan Projects of China (Grant No. 2013BAC05B01), the Key Scientific and Technological Project of Henan Province (Grant No. 212102310433), the Key research Project of higher education institutions in Henan Province (Grant No. 20A170012), the National Nature Science Foundation of China (Grant Nos. 32001250 and 42071198) and University Science and Technology Innovation Team of Henan Province (Grant No. 23IRTSTHN017). Part data used in this paper are acquired by National Science & Technology Infrastructure of China, Data Sharing Infrastructure of Earth System Science -Data Center of Lower Yellow River Regions (http://henu.geodata.cn). We want to provide our gratitude to the editors and the anonymous reviewers.

Conflict of Interest

The authors declare no conflict of interest.

References

1. HOU T., ZHU Y., LU H., SUDICKY E., YU Z., & OUYANG, F. Parameter sensitivity analysis and optimization of noah land surface model with field measurements from huaihe river basin, china. Stochastic Environmental Research and Risk Assessment, **29** (5), 1383, **2015**.
2. SONG X., ZHANG J., ZHAN C., XUAN Y., YE M., XU C. Global sensitivity analysis in hydrological modeling: Review of concepts, methods, theoretical framework, and applications. Journal of Hydrology, **523**, 739, **2015**.
3. WANG X., QIAN W., JUAN D.U., WENG Y. Sensitivity analysis of calculus of variations and its application in distributed hydrological models. Journal of Sichuan University of Science Engineering (Natural Science Edition), **2015**.
4. WU H. Integrated sensitivity analysis, calibration, and uncertainty propagation analysis approaches for supporting hydrological modeling. Memorial University of Newfoundland, **2016**.
5. XU X., SUN C., HUANG G., MOHANTY B.P. Global sensitivity analysis and calibration of parameters for a physically-based agro-hydrological model. Environmental Modelling Software, **83**, 882, **2016**.
6. STAHN P., BUSCH S., SALZMANN T., EICHLER-LOEBERMANN B., MIEGEL K. Combining global sensitivity analysis and multiobjective optimisation to estimate soil hydraulic properties and representations of various sole and mixed crops for the agro-hydrological swap model. Environmental Earth ences, **76** (10), **2017**.
7. SINGH V., GOYAL M.K. Curve number modifications and parameterization sensitivity analysis for reducing model uncertainty in simulated and projected streamflows in a himalayan catchment. Ecological Engineering, 108, **2017**.
8. HUANG J., WEN J., WANG B., HINOKIDANI O. Parameter sensitivity analysis for a physically based distributed hydrological model based on morris' screening method. Journal of Flood Risk Management, **13** (1), **2020**.
9. SHENG S., CHEN H., LIN K., XU C., GUO S. Parameters sensitivity analysis of the xin'anjiang model under different temporal and spatial scales. Journal of Water Resources Research, **07** (06), **2018**.
10. LIU S., SHE D.X., ZHANG L.P., DING K.X., GUO M.Y., CHEN S.L. Global Sensitivity Analysis of Hydrological Model Parameters Based on Morris and Sobol Methods. Resources and Environment in the Yangtze Basin, **8** (6), **2019**.
11. LIU H., DAI H., NIU J., HU B.X., GUI D., QIU H., YE M., CHEN X., WU C., ZHANG J., RILEY W. Hierarchical sensitivity analysis for a large-scale process-based hydrological model applied to an Amazonian watershed. Hydrology and Earth System Sciences, **24** (10), **2020**.
12. UKI V., RADI Z. Sensitivity analysis of a physically based distributed model. Water Resources Management, **30** (5), 1669, **2016**.
13. OLIVEIRA A.R., RAMOS T.B., SIMIONESEI L., PINTO L., NEVES R. Sensitivity analysis of the mohid-land

hydrological model: A case study of the ulla river basin. In Water (Switzerland), **12** (11), **2020**.
14. VERMA M.K., VERMA M.K. Calibration of a hydrological model and sensitivity analysis of its parameters: A case study of Seonath river basin. International Journal of Hydrology Science and Technology, **9** (6), **2019**.
15. LIU Y., LIU J., LI C., YU F., QIU Q. Parameter Sensitivity Analysis of the WRF-Hydro Modeling System for Streamflow Simulation: a Case Study in Semi-Humid and Semi-Arid Catchments of Northern China. Asia-Pacific Journal of Atmospheric Sciences, **57** (3), **2020**.
16. ZHANG J.L., YONG-PING L.I., ZENG X.T., YOU L., LIU J. Hydrological parameter sensitivity analysis for a cold and arid watershed based on EFAST. South-to-North Water Transfers and Water Science Technology, **15** (3), 6, **2017**.
17. HAGHNEGAHDAR A., RAZAVI S., YASSIN F., WHEATER H. Multicriteria sensitivity analysis as a diagnostic tool for understanding model behaviour and characterizing model uncertainty. Hydrological Processes, **31** (25), 4462, **2017**.
18. VEIHE A., QUINTON J. Sensitivity analysis of eurosem using monte carlo simulation i: hydrological, soil and vegetation parameters. Hydrological Processes, **14** (5), 915, **2015**.
19. GAN Y., LIANG X.Z., DUAN Q., CHOI H.I., DAI Y., WU H. Stepwise sensitivity analysis from qualitative to quantitative: application to the terrestrial hydrological modeling of a conjunctive surface-subsurface process (cssp) land surface model. Journal of Advances in Modeling Earth Systems, **7** (2), 648, **2015**.
20. WANG C.X., CHEN M., YONG-PING L.I. Polynomial Chaos Expansion Method for Parameters Sensitivity Analysis of Hydrological Model. Water Resources and Power, **34** (10), 5, **2016**.
21. STAVROPULOS-LAFFAILLE X., CHANCIBAULT K., ANDRIEU H., LEMONSU A., MASSON V. Hydrological validation of an urban hydro-microclimate model (teb-hydro): sensitivity analysis on the catchment of reze (nantes, france). Houille Blanche (3), 14, **2017**.
22. HUANG J., WEN J., WANG B., ZHOU Q., OSAMU H., HYDRAULIC S.O., AMP E., ENGINEERING P., UNIVERSITY Y. Application of parameter sensitivity analysis for a physically based distributed hydrological model in the Bukuro river basin. Journal of Yangzhou University (Natural Science Edition), **21** (4), 72, **2018**.
23. PENG T., TANG Z., YIN Z., DING H. Hydrological Simulation and Parameter Sensitivity Analysis of Small and Medium Basins in the Western Mountains of Hubei Province. Advances in Meteorological Science and Technology, **8** (4), 6, **2018**.
24. JIN H., JU Q., YU Z., HAO J., LI W. Simulation of snowmelt runoff and sensitivity analysis in the nyang river basin, southeastern qinghai-tibetan plateau, china. Natural Hazards, **99** (2), 931, **2019**.
25. SILVA M., NETTO A.D.O.D.A., NEVES R., VASCO A., FACCIOLI G.G. Sensitivity analysis and calibration of hydrological modeling of the watershed northeast brazil. Journal of Environmental Protection, **06** (8), 837, **2015**.
26. POHL E., KNOCHE M., GLOAGUEN R., ANDERMANN C., KRAUSE P. Sensitivity analysis and implications for surface processes from a hydrological modelling approach in the gunt catchment, high pamir mountains. Earth Surface Dynamics, **3** (3), 333, **2015**.
27. ZIEHER T., RUTZINGER M., SCHNEIDER-MUNTAU B., PERZL F., LEIDINGER D., FORMAYER H. Sensitivity analysis and calibration of a dynamic physically based slope stability model. Natural Hazards Earth System Sciences, **17** (6), 1, **2017**.
28. YANG X., JOMAA S., RODE M. Sensitivity analysis of fully distributed parameterization reveals insights into heterogeneous catchment responses for water quality modeling. Water Resources Research, **55** (12), **2019**.
29. TING Y., HYONGKI L., HAHN J. Toward estimating wetland water level changes based on hydrological sensitivity analysis of palsar backscattering coefficients over different vegetation fields. Remote Sensing, **7** (3), 3153, **2015**.
30. GIUDICE G.D., PADULANO R. Sensitivity analysis and calibration of a rainfall-runoff model with the combined use of epa-swmm and genetic algorithm. Acta Geophysica, **64** (5), 1755, **2016**.
31. MA Q., ZAVATTERO E., DU M., VO N.D., GOURBESVILLE P. Assessment of high resolution topography impacts on deterministic distributed hydrological model in extreme rainfall-runoff simulation. Procedia Engineering, **154**, 601, **2016**.